

Tympanotonus fuscatus and *Crassostrea gasar* Shells Mediated Synthesis of Silver Nanoparticles

Babatunde T. Ogunyemi¹ Ogunyemi O. Oderinlo¹ Taye Temitope Alawode*

Received: 29 July 2024/Accepted: 16 October 2024/Published: 26 October 2024

Abstract: *This study presents a comparative analysis of silver nanoparticles synthesized via green methods using two different plant extracts, identified as TF-NP and CG-NP. Scanning Electron Microscopy (SEM) and particle size distribution analysis were employed to evaluate the morphology and size of the nanoparticles. The SEM image of TF-NP revealed uniformly dispersed, spherical nanoparticles with minimal agglomeration and a measured average size predominantly ranging between 30 and 60 nm. In contrast, CG-NP exhibited irregular, flake-like structures with significant aggregation, and particle sizes ranging widely from 0.55 μm to over 17 μm , with the majority falling above the nanoscale threshold. Histogram analysis further confirmed that 60% of TF-NP particles were below 60 nm, while CG-NP had less than 10% of particles within the nanoscale range. The findings indicate that the TF-NP synthesis process resulted in nanoparticles that align more closely with international nanoparticle standards, due to better control of synthesis parameters and the presence of more effective phytochemicals in the plant extract. In contrast, CG-NP synthesis demonstrated limited efficiency and poor size control. The study concludes that the choice of plant extract significantly influences the quality of green-synthesized nanoparticles, and it recommends further optimization of the synthesis protocol for CG-NP to improve particle uniformity and reduce agglomeration.*

Keywords: *Silver nanoparticles (AgNPs) , Green synthesis, SEM analysis, Particle size distribution, Phytochemical reduction*

Babatunde T. Ogunyemi*

Department of Chemistry, Federal University Otuoke, Bayelsa State, Nigeria

Email: ogunyemibt@fuotuoke.edu.ng

Orcid id:0000-0002-3634-488X

Ogunyemi O. Oderinlo

Department of Chemistry, Federal University Otuoke, Bayelsa State, Nigeria

Email: oderinlooo@fuotuoke.edu.ng

Orcid id: 0000-0002-6180-5502

Taye Temitope Alawode*

Department of Chemistry, Federal University Otuoke, Bayelsa State, Nigeria

Email: Onatop@gmail.com

Orcid id: 0000-0002-8671-8632

1.0 Introduction

Silver nanoparticles (AgNPs), typically ranging from 1 to 100 nm in size, possess remarkable physical, chemical, and biological characteristics owing to their high surface area-to-volume ratio and their ability to absorb and scatter light across the visible and near-infrared spectrum (Altammar, 2023). These properties have enabled their widespread application across diverse fields including agriculture, environmental monitoring, medicine, biotechnology, and the food industry. Specifically, AgNPs have demonstrated utility in wastewater treatment (Zahra et al., 2020), environmental surveillance (Eddy et al., 2024a; Rassaei et al., 2011), antimicrobial treatments (Islam et al., 2022), and as functional additives in food products (Chen et al., 2023).

Various methods exist for the synthesis of silver nanoparticles, including physical, chemical, and biological approaches (Akpanudo & Olabemiwo, 2024a). Among these, biological (or green) synthesis is

increasingly favored due to its eco-friendliness, simplicity, and economic viability (Ijaz et al., 2022). This method typically employs natural reducing and stabilizing agents derived from plant extracts, microorganisms, and biowastes. However, while green synthesis has gained traction globally, the bulk of existing research remains focused on terrestrial plant-based materials, with marine-derived biowastes receiving considerably less attention.

Nigeria, with its extensive coastline and rich marine biodiversity, generates an estimated 12 million tonnes of shell waste annually—primarily composed of oyster and periwinkle shells (Mo et al., 2018; Eddy et al., 2024b-e). These shells, often discarded indiscriminately along shores and in landfills, pose environmental and public health hazards due to poor waste management practices (Barros et al., 2009). Yet, they remain a largely untapped resource for nanotechnology applications. Mollusk shells are organo-mineral composites, consisting of 95–99% inorganic minerals and 0.1–5% organic materials. Though minor in proportion, the organic matrix—rich in proteins, polysaccharides, and lipids—has the capacity to act as natural reducing and capping agents in nanoparticle synthesis (Ma et al., 2006).

Despite their abundance and biochemical richness, oyster and periwinkle shells have been underutilized in green nanotechnology research. Most reported studies emphasize plant-based precursors, thereby leaving a significant knowledge gap in the exploration of marine biowastes as sustainable alternatives for nanoparticle synthesis. Addressing this gap is imperative for promoting resource recovery and environmental sustainability.

This study therefore aims to synthesize and characterize silver nanoparticles using ethyl acetate extracts of *Tympanotonus fuscatus* and *Crassostrea gasar* shells. By investigating the potential of these marine-derived wastes, the study seeks to advance the development of cost-effective, eco-friendly nanomaterials

while promoting sustainable management of marine biowaste.

2.0 Materials and Methods

Periwinkle (*Tympanotonus fuscatus*) and oyster (*Crassostrea gasar*) shells were collected from the Otuoke market located in Ogbia Local Government Area, Bayelsa State, Nigeria. These marine mollusks are widely consumed in the Niger Delta region, and their shells are typically discarded as waste. The sampling site was selected due to its accessibility and the high volume of shellfish waste generated in the area.

2.2 Preparation of Periwinkle and Oyster Shell Extracts

Collected shells were first rinsed thoroughly under running tap water to remove residual organic matter, followed by washing with distilled water to eliminate surface impurities and contaminants. The clean shells were then air-dried at room temperature for 72 hours to prevent microbial degradation. Dried shells were ground into a fine powder using a mechanical grinder and sieved to achieve uniform particle size.

An 8 g sample of each powdered shell type was extracted separately in 100 mL of ethyl acetate using reflux boiling in a 250 mL Erlenmeyer flask for 30 minutes at 60°C. Ethyl acetate was selected as the solvent due to its efficiency in extracting bioactive compounds such as esters, flavonoids, and fatty acids, which can act as natural reducing and capping agents. After extraction, each mixture was filtered through Whatman No. 1 filter paper, and the clear filtrates were stored in amber-colored bottles at 4°C to prevent photodegradation before use in nanoparticle synthesis.

2.3 Synthesis of Silver Nanoparticles

To synthesize the silver nanoparticles (AgNPs), 15 mL of each shell extract was mixed separately with 85 mL of 1 mM aqueous silver nitrate (AgNO_3) solution. The mixtures were stirred gently and incubated at 28°C for 3 hours in the dark to prevent photo-reduction of silver ions. The onset of nanoparticle formation was



confirmed by a visible color change from pale yellow to deep brown, attributed to the surface plasmon resonance (SPR) of AgNPs. This color transition indicates the reduction of Ag^+ ions to Ag^0 nanoparticles by the organic components in the shell extract.

2.4 Characterisation of Synthesised Silver Nanoparticles

The ethyl acetate extracts and the synthesized AgNPs were subjected to characterization using:

Fourier Transform Infrared (FTIR) Spectroscopy: To identify the functional groups in the shell extracts responsible for reduction and stabilization of the AgNPs. The FTIR spectra were recorded in the range of $4000\text{--}400\text{ cm}^{-1}$ to determine the presence of hydroxyl, carbonyl, amine, and other bioactive moieties.

Scanning Electron Microscopy (SEM): To examine the surface morphology, size, and shape of the synthesized AgNPs. SEM images provided detailed microstructural insights, enabling determination of nanoparticle dispersion and agglomeration behavior.

4.0 Results and Discussion

Fourier Transform Infrared (FTIR) Spectral Analysis of Shell Extracts and Synthesized Silver Nanoparticles

FTIR spectroscopy was employed to identify the bioactive functional groups responsible for

the reduction and stabilization of silver nanoparticles (AgNPs) synthesized using shell extracts of *Tympanotonus fuscatus* and *Crassostrea gasar*. The spectra of both the ethyl acetate extracts and the corresponding silver nanoparticles were analyzed and compared to elucidate the role of specific chemical moieties in nanoparticle synthesis.

Fig. 1A shows the FTIR spectrum of the *Tympanotonus fuscatus* ethyl acetate extract (TFEE). A broad absorption peak observed at 3458 cm^{-1} is attributed to O–H stretching vibrations, typical of hydrogen-bonded alcohols or phenolic compounds. This suggests the presence of hydroxyl-containing biomolecules, which are known to participate in the reduction of metal ions. Another prominent band at 1738 cm^{-1} corresponds to the C=O stretching of esters or carboxylic acids. This functional group is indicative of lipid or fatty acid derivatives, which also have reducing potential. A notable band at 1637 cm^{-1} is due to C=C stretching vibrations associated with alkenes or aromatic compounds, while the band at 1032 cm^{-1} is ascribed to C–O stretching vibrations from esters, ethers, or alcohols. These observations collectively point to the presence of biomolecules capable of acting as reducing and capping agents in the green synthesis of silver nanoparticles.

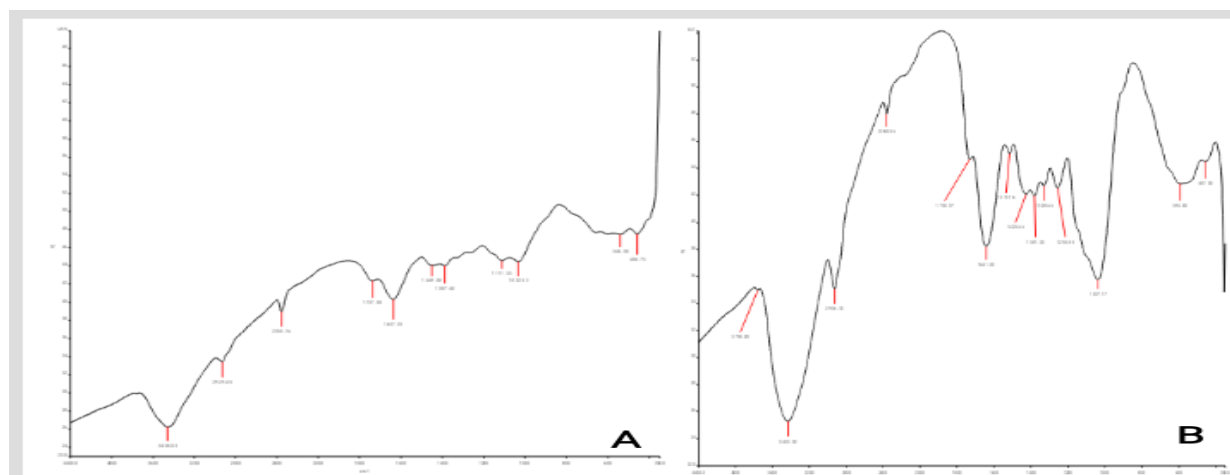


Fig. 1: FTIR spectra of ethyl acetate extract of (A) *T. fuscatus* shell (A) and (B) the synthesized silver nanoparticles



Upon synthesis of the silver nanoparticles using the *T. fuscatus* extract, the FTIR spectrum of the resulting nanoparticles (TFNP), as shown in **Fig. 1B**, revealed some distinct changes. The O–H stretching band appeared at a slightly lower wavenumber (3433 cm^{-1}), suggesting the involvement of hydroxyl groups in binding to silver ions. Similarly, the C=O stretching band shifted from 1738 cm^{-1} in the extract to 1730 cm^{-1} in the nanoparticles, implying interaction of the carbonyl moieties with silver during nanoparticle formation. A new peak emerged at 1381 cm^{-1} , which may be attributed to nitro or nitrous functional groups, possibly formed during the redox reaction between the extract biomolecules and silver

ions. These spectral changes confirm the role of bioactive compounds in TFEE as both reducing agents and stabilizers of silver nanoparticles.

In the case of *Crassostrea gasar*, the FTIR spectrum of its ethyl acetate extract (CGEE), presented in **Fig. 2A**, displayed less intense but distinct absorption bands. The spectrum showed a moderate peak at 1600 cm^{-1} , associated with C=C stretching vibrations, and a sharp band at 1027 cm^{-1} , indicative of C–O stretching from alcohols or esters. These suggest that similar functional groups to those in TFEE are present in CGEE, although likely in lesser concentration or with reduced structural complexity.

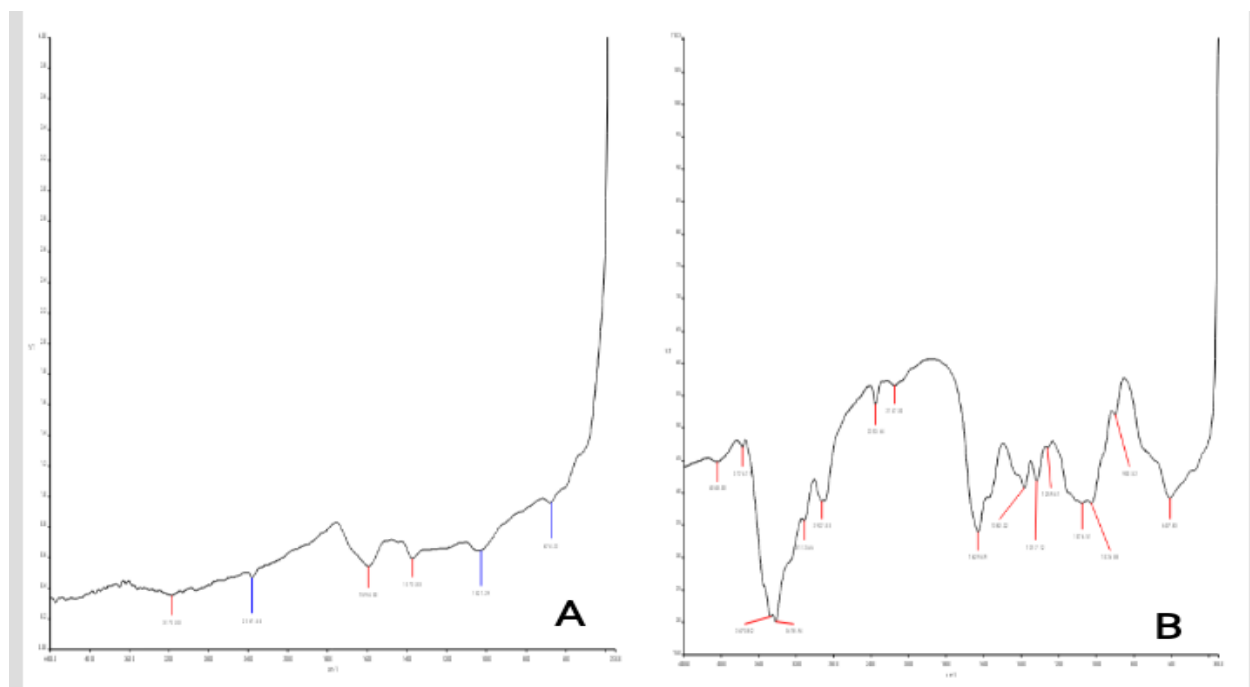


Fig. 4: FTIR spectra of ethyl acetate extract of *C. gasar* shell (A) and the synthesized nanoparticles from *C. gasar* shell (B)

After the synthesis of silver nanoparticles using *C. gasar* extract, the FTIR spectrum of the resulting CGNP, shown in **Fig. 2B**, exhibited significant changes. A broad band in the range of $3470\text{--}3418\text{ cm}^{-1}$ was observed, corresponding to N–H stretching of primary amides, which were absent in the original extract spectrum. This suggests the incorporation or exposure of proteinaceous materials during nanoparticle synthesis. The

appearance of a strong band at 1640 cm^{-1} is attributed to the C=O stretching vibration of amide groups, further supporting the involvement of proteins or peptides in the stabilization of the nanoparticles. As in the case of TFNP, a band at 1381 cm^{-1} was also observed, again indicating the presence of nitrous functional groups possibly arising from complexation or rearrangement reactions during synthesis.



A comparative analysis of the FTIR data for all four samples (TFEE, TFNP, CGEE, and CGNP) is summarized in **Table 1**. This table presents the observed FTIR peaks alongside standard reference values and their

corresponding functional group assignments. It highlights the key differences between the extract and nanoparticle spectra, underscoring the functional groups most likely involved in the reduction and stabilization processes.

Table 1: FTIR Peak Assignments and Functional Group Interpretation for Extracts and Synthesized Silver Nanoparticles

Sample	Observed Peak (cm ⁻¹)	Reference Value (cm ⁻¹)	Functional Group	Interpretation
TFEE	3458	3200–3600	O–H (alcohol/phenol)	Hydrogen bonding; involved in reduction
TFEE	1738	1700–1750	C=O (ester)	Likely involved in reducing/stabilizing AgNPs
TFEE	1637	1620–1680	C=C (alkenes/aromatic)	Electron-rich sites; possible reducing agents
TFEE	1032	1000–1300	C–O (ester/ether/alcohol)	Present in capping molecules
TFNP	3433	3200–3600	O–H	Shifted from extract; suggests nanoparticle interaction
TFNP	1730	1700–1750	C=O (ester)	Binding to silver; slight shift observed
TFNP	1381	1350–1390	NO ₂ (nitro/nitrous)	New peak; formed during Ag ⁺ interaction
CGEE	1600	1600–1680	C=C	Present in alkenes or aromatic compounds
CGEE	1027	1000–1300	C–O	Present in polysaccharides or esters
CGNP	3418–3470	3300–3500	N–H (primary amide)	New peak; indicates proteinaceous capping
CGNP	1640	1600–1700	C=O (amide)	Peptide/protein involvement
CGNP	1381	1350–1390	NO ₂	Present in synthesized nanoparticles

The FTIR analysis demonstrates that the biosynthesis of silver nanoparticles using *T. fuscatus* and *C. gasar* ethyl acetate extracts is mediated by biomolecules containing hydroxyl, carbonyl, and nitro functional groups. The shift in peak positions and the appearance of new functional group absorptions, particularly nitrous and amide moieties, support the conclusion that these groups are directly involved in the reduction of Ag⁺ to Ag⁰ and the subsequent stabilization of the nanoparticles. These findings underscore

the green and biologically active nature of the synthesis process and highlight the importance of functional group interactions in nanoparticle formation.

3.2 Characterization and Particle Size Analysis of Synthesized Silver Nanoparticles

The synthesized silver nanoparticles were characterized using Scanning Electron Microscopy (SEM) and particle size distribution analysis to evaluate their morphology and size range. The SEM micrograph of TF aided AgNPs (Fig. 3),



captured at a magnification of 12,000 \times and an accelerating voltage of 20 kV, reveals well-dispersed, compact, and predominantly spherical nanoparticles. The particles exhibit minimal aggregation, suggesting that the reducing and capping agents present in the plant extract used for synthesis were effective in producing stabilized nanoparticles. The uniformity in shape and size implies a controlled nucleation and growth process, likely influenced by the phytochemical constituents of the plant. This morphology is favorable for applications that require a consistent surface area, such as in catalysis or antimicrobial coatings. In contrast, the SEM micrograph of CG aided AgNPs (Fig. 4), also

taken at a magnification of 12,000 \times but with a slightly lower accelerating voltage of 15 kV, displays a different morphology. The particles appear as flake-like aggregates with uneven surfaces and irregular distribution. This structural heterogeneity suggests a lower degree of stabilization during synthesis, possibly due to less effective phytochemicals or suboptimal reaction parameters such as temperature, pH, and duration. The presence of agglomerates indicates particle fusion and uncontrolled growth, which can reduce the effectiveness of the nanoparticles in applications that depend on nanoscale properties.

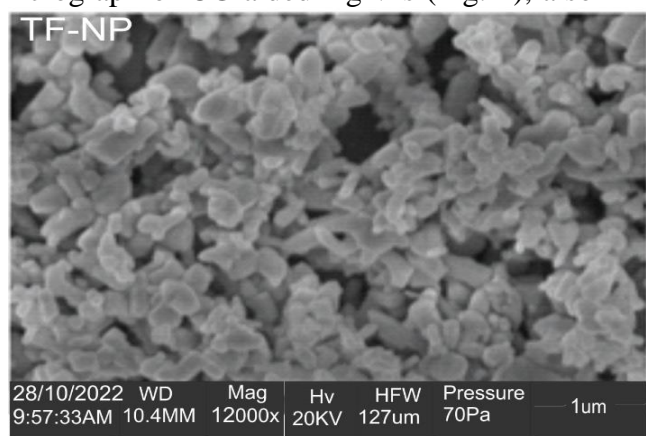


Fig. 3: SEM Analysis of AgNPs Synthesized from AgNO₃ using *T. fuscatus* (TF) Shell Extract

The particle size distribution of TF aided AgNPs (Fig. 5) provides further insights into the quality of the synthesis. A histogram analysis indicates that the majority of particles fall within the range of 0.03 to 0.06 μm , with the highest frequency recorded in this size bracket. There is a notable secondary peak between 0.10 and 0.11 μm , but the overall distribution remains relatively narrow. This confirms that most of the TF aided AgNO₃ particles are within the 30–60 nm size range, which places them well within the nanoscale definition provided by ISO/TS 80004-1:2015, which classifies nanoparticles as materials with dimensions between 1 and 100 nm. Such a narrow and uniform distribution reflects

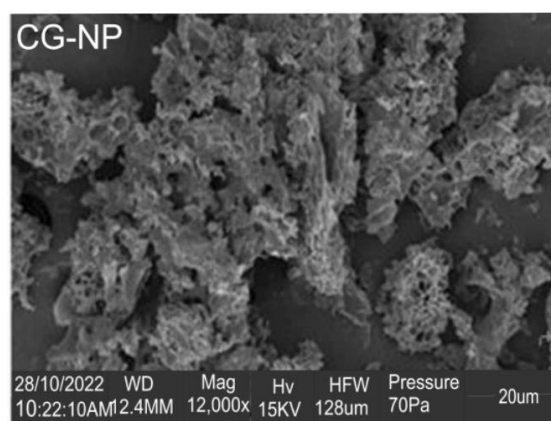


Fig. 4: SEM Analysis of AgNPs Synthesized AgNO₃ using *C. gasar* (CG) Shell Extract

precise control over the synthesis process and suggests the particles are well suited for applications in drug delivery, electronics, or environmental remediation.

On the other hand, the particle size distribution for CG-NP reveals a much broader and skewed pattern. The histogram shows a dominant size population between 0.15 μm and 0.75 μm , with particle sizes extending beyond 17 μm . This distribution suggests significant aggregation and growth beyond the nanoscale, with most particles falling in the submicron to micrometer range. These results are consistent with the SEM micrograph observations, confirming that



the synthesis process for CG aided AgNPs (Fig. 6) was not effectively controlled. Such particle sizes are not suitable for applications where a high surface-to-volume ratio is critical, such as

in biosensing or nanomedicine. Instead, these particles might find better use in bulk applications, such as adsorbents in environmental cleanup.

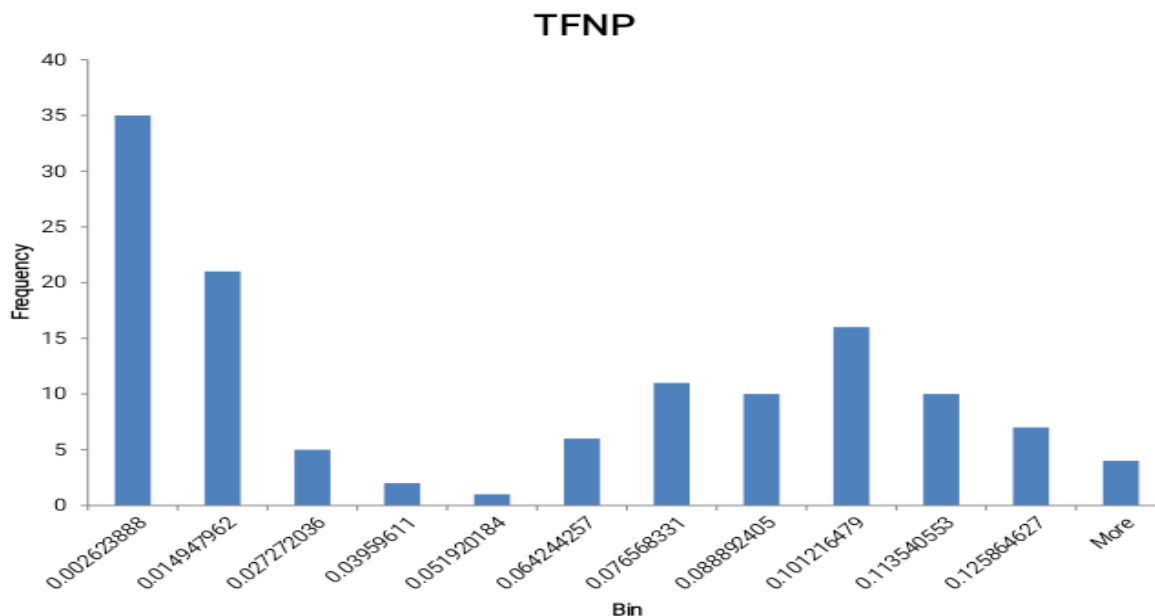


Fig. 5: Particle Size distribution of Nanoparticles Synthesized from T. fuscatus Shell Extract

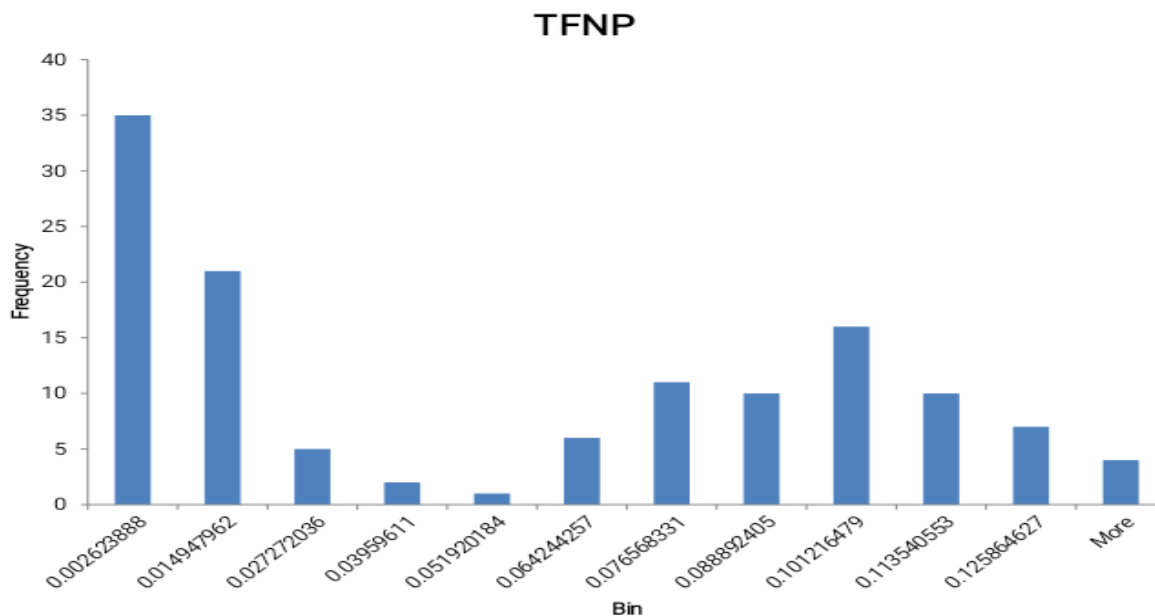


Fig. 6: Particle Size distribution of Nanoparticles Synthesized from T. fuscatus Shell Extract

When comparing the two nanoparticle types, TF aided AgNPs demonstrate superior synthesis characteristics with spherical morphology, narrow particle size distribution, and particle sizes within the nanometer range. In contrast, CG-NP exhibits irregular

morphology, broad distribution, and particle sizes largely outside the nanoscale range. These differences highlight the importance of selecting appropriate plant materials and optimising reaction conditions during green synthesis. Compared with literature values, TF



aided AgNPs aligns well with standards for green-synthesised silver nanoparticles. For example, Ahmad et al. (2010) and Roy and Das (2020) reported effective AgNPs synthesized using plant extracts, typically within the 10–50 nm range, showing strong antibacterial and catalytic activity. TF-NP falls within this optimal range, supporting its potential for high functional performance. Conversely, the particle characteristics of CG-NP resemble those described by Chatterjee et al. (2016), where insufficient stabilization led to aggregation and particle sizes beyond 1 μm , thereby diminishing their effectiveness for nanoscale applications.

In conclusion, the SEM and particle size analyses clearly demonstrate that TF-NP possesses the desirable characteristics of a well-synthesized silver nanoparticle, including controlled size, shape, and dispersion. CG-NP, however, requires further optimization to achieve comparable quality. The results emphasize the need to tailor synthesis parameters according to the phytochemical profile of the source plant and intended application of the nanoparticles.

4.0` Conclusion

The characterization and analysis of the synthesized silver nanoparticles revealed significant differences in morphological features and particle size distribution between the two samples, TF-NP and CG-NP. The TF-NP sample exhibited a well-defined spherical shape with uniform dispersion and minimal aggregation, as observed from the SEM image. Its particle size distribution showed a narrow range, predominantly between 30 and 60 nanometers, confirming successful synthesis within the nanoscale. In contrast, the CG-NP sample displayed irregular, flake-like morphologies with extensive agglomeration, and its particle size distribution ranged from submicron to over 17 micrometers, far exceeding the standard nanoscale limits. These results suggest that the synthesis of TF-NP was more efficient and better controlled, likely due

to more effective phytochemical constituents in the plant extract and optimized reaction conditions.

In conclusion, TF-NP proved to be a superior product in terms of structural integrity, size uniformity, and compatibility with the definition of nanoparticles. The CG-NP, however, demonstrated poor control over particle size and morphology, reducing its suitability for applications that depend on nanoscale properties. These findings underscore the critical role of plant extract composition, reaction parameters, and synthesis strategy in achieving desirable nanoparticle characteristics.

It is recommended that future synthesis of CG-NP be optimized by modifying key reaction parameters such as pH, temperature, and extract concentration, or by exploring other plant sources with stronger reducing and stabilizing capabilities. Additional purification steps or post-synthesis treatments may also be employed to reduce particle aggregation. The successful synthesis of TF-NP supports the potential of green synthesis methods as sustainable and effective approaches for producing high-quality silver nanoparticles for use in medical, environmental, and industrial applications. Further studies are encouraged to investigate the functional properties of the synthesized nanoparticles, including their antimicrobial efficacy, catalytic activity, and environmental stability.

5.0 References

- Akpanudo, N. W., & Olabemiwo, O. M. (2024a). Synthesis and characterization of silver nanoparticles and nanocomposites using *Echinochloa pyramidalis* (Antelope grass) plant parts and the application of the nanocomposite... *South African Journal of Chemical Engineering*, 47, 1, pp. 98-110.
- Akpanudo, N. W., & Olabemiwo, O. M. (2020b). Green synthesis and characterization of copper nanoparticles (CuNPs) and composites (CuC) using the *Echinochloa pyramidalis* extract and their



- application in... *Water Practice & Technology*, 19, 2, pp. 324-342.
- Altammar K A. (2023). A review on nanoparticles: characteristics, synthesis, applications, and challenges. *Front Microbiol.* 2023 Apr 17;14:1155622. doi: 10.3389/fmicb.2023.
- Eddy, N. O., Garg, R., Garg, R., Garg, R., Ukpe, R. A. & Abugu, H. (2024a). Adsorption and photodegradation of organic contaminants by silver nanoparticles: isotherms, kinetics, and computational analysis. *Environ Monit Assess*, 196, 65, <https://doi.org/10.1007/s10661-023-12194-6>.
- Eddy, N. O., Oladede, J., Eze, I. S., Garg, R., Garg, R., & Paktin, H. (2024b). Synthesis and characterization of CaO nanoparticles from periwinkle shell for the treatment of tetracycline-contaminated water by adsorption and photocatalyzed degradation. *Results in Engineering*, 103374. <https://doi.org/10.1016/j.rineng.2024.103374>.
- Eddy, N. O., Jibrin, J. I., Ukpe, R. A., Odiongenyi, A., Iqbal, A., Kasiemobi, A. M., Oladele, J. O., & Runde, M. (2024c). Experimental and Theoretical Investigations of Photolytic and Photocatalysed Degradations of Crystal Violet Dye (CVD) in Water by oyster shells derived CaO nanoparticles (CaO-NP), *Journal of Hazardous Materials Advances*, 13, 100413, <https://doi.org/10.1016/j.hazadv.2024.100413>.
- Eddy, N. O., Garg, R., Ukpe, R. A., Ameh, P. O., Gar, R., Musa, R., Kwanchi, D., Wabaidur, S. M., Afta, S., Ogbodo, R., Aikoye, A. O., & Siddiqu, M. (2024d). Application of periwinkle shell for the synthesis of calcium oxide nanoparticles and in the remediation of Pb²⁺-contaminated water. *Biomass Conversion and Biorefinery*, doi: 10.1007/s13399-024-05285-y.
- Eddy, N. O., Garg, R., Garg, R., Ngwu, C., Ekele, D. O., Awe, F. E., Ukpe, R. A. & Ogbonna, I. (2024e). Experimental and theoretical investigations of crab shell-based CaO nanoparticles for the photodegradation of penicillin G in water. *International Journal of Environmental Science and Technology* DOI: 10.1007/s13762-024-06214-2.
- Barros, M. C., Bello, P. M., Bao, M. & Torrado J. J. (2009). From waste to commodity: transforming shells into high purity calcium carbonate. *Journal of Cleaner Production*, 17, 3, pp. 400-407. doi:10.1016 -/j.jclepro.2008.08.013.
- Chen, J., Guo, Y., Zhang, X., Liu, J., Gong, P., Su, Z. et al. (2023). Emerging nanoparticles in food: sources, application, and safety. *J. Agricult. Food Chem.* 71, pp. 3564–3582.
- Ijaz, I., Bukhari, A, Gilani, E., Nazir, A., Zain, H., Saeed, R., Hussain, S., Hussain, T., Bukhari, A., Naseer, Y. & Aftab, R. (2022). Green synthesis of silver nanoparticles using different plants parts and biological organisms, characterization and antibacterial activity. *Environmental Nanotechnology, Monitoring & Management*, 18, 100704, <https://doi.org/10.1016/j.enmm.2022.100704>.
- Islam, F., Shohag, S., Uddin, M. J., Islam, M. R., Nafady, M. H., Akter, A., et al. (2022). Exploring the journey of zinc oxide nanoparticles (ZnO-NPs) toward biomedical applications. *Materials* 15, 6, 2160, doi: 10.3390/ma15062160
- Ma, H. Y. & Lee, I. S.(2006).Characterization of vaterite in low quality freshwater-cultured pearls. *Mater. Sci. Eng.C* 26, pp. 721-723. doi:10,1016/j.msec.2005.09.109
- Mo, K. H., Alengaram, U. I., Jumaat, M. Z., Lee, S. C., Goh, W. I. & Yuen, C. W. . (2018). Recycling of seashell waste in concrete: A review, construction and building materials.162, pp. 751-764.



doi:10.1016/J.CONBUILDMAT.2017.12.009

Rassaei, L., Marken, F., Sillanpää, M., Amiri, M., Cirtiu, C. M. & Sillanpää, M. (2011). Nanoparticles in electrochemical sensors for environmental monitoring. *TrAC Trends Anal. Chem.* 30, pp. 1704–1715.

Zahra, Z., Habib, Z., Chung, S. & Badshah, M. A. (2020). Exposure route of TiO₂ NPs from industrial applications to wastewater treatment and their impacts on the agro-environment. *Nanomaterials* doi: 10:1469.10.3390/nano10081469.

Declaration

Consent for publication

Not applicable

Availability of data

Data shall be made available on demand.

Competing interests

The authors declared no conflict of interest

Ethical Consideration

Not applicable

Funding

There is no source of external funding.

Authors' contributions

BT Ogunyemi and TT Alawode designed the project, OO Oderinlo and TT Alawode carried out the synthesis. All the authors analyzed the data and prepared the manuscript.

